A

Sample	n	Input	CpGs (1X)	Unique (1X)	Mean Coverage (1X)	r
NB	3	30 per replicate	40224734	1667058	21.5	0.82
P10	3	10 per replicate	76649439	2177472	35.1	0.80
P60	2	3-5 per replicate	107917886	2397229	45.0	0.90

B

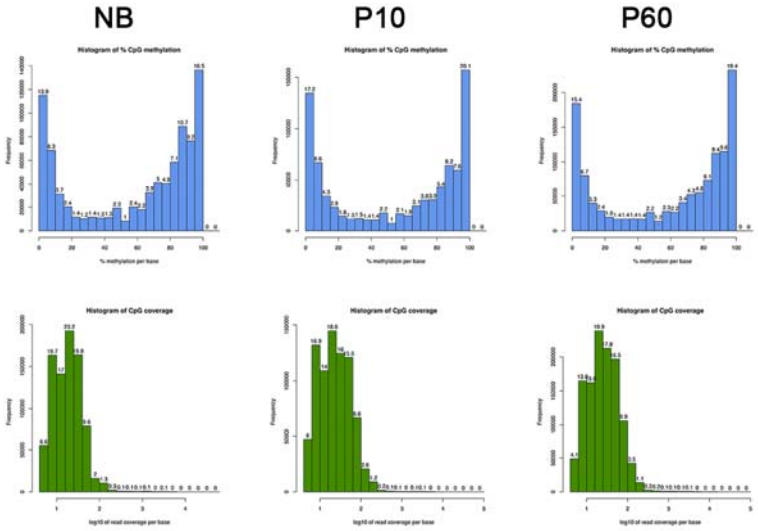

C

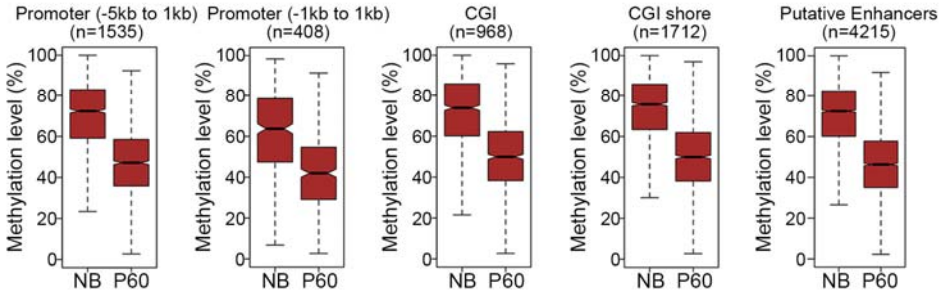

D

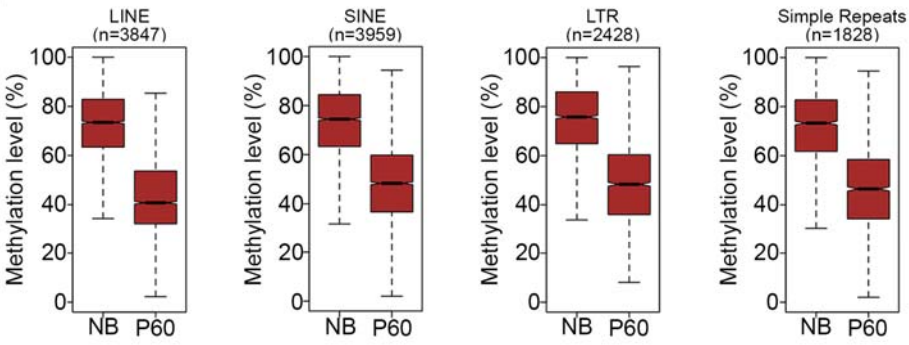

Figure S1, related to Figure 1

Figure S1: RRBS basic statistics, related to Figure 1

(**A**) Table of CpG coverage captured by RRBS showing the number of replicates (*n*), input (number of mice used for sciatic nerve isolation), numbers of total and unique CpGs covered at least once (1X), mean coverage and mean Pearson´s correlation (*r*) between the replicates for each stage. (**B**) Distribution histograms of CpG methylation levels showing expected bimodal DNA methylation pattern (*upper panels*). *Bottom panels* showing that the vast majority of cytosines measured have excellent coverage (at least 5 valid reads). A representative replicate of each of the 3 time-points analyzed is shown. (**C**,**D**) Boxplots showing percentage methylation levels of all differentially-methylated 1-kb tiling regions (q<0.05, methylation difference of 20%), mapped to (**C**) gene-regulatory regions, and (**D**) repeat elements. Number of genomic sites (*n*) is indicated.

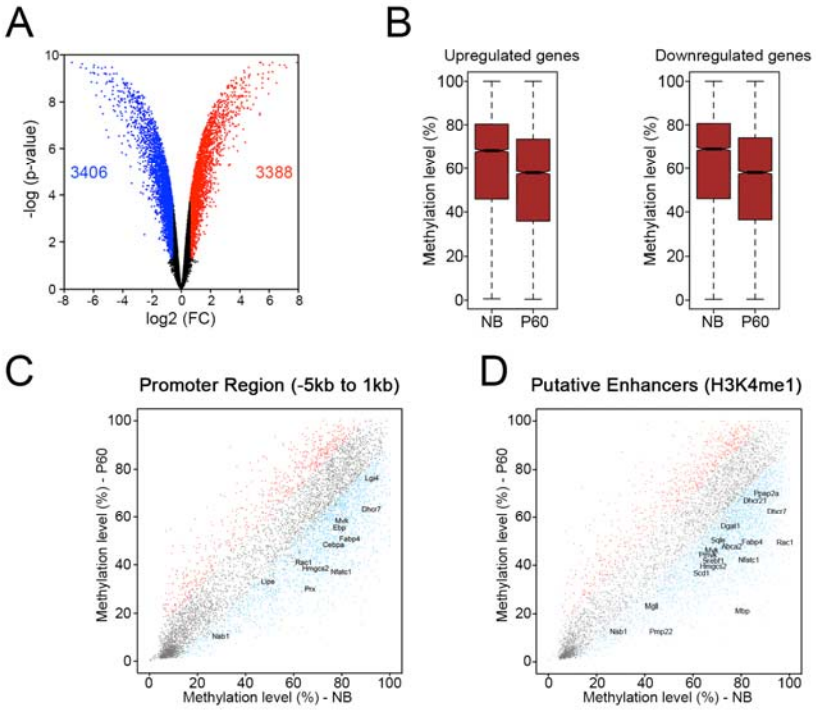

E

	Upregulated Genes (ALL) n=3410	Upregulated Genes (Lipid Metabolism Category) n=352
1kb Tiles	*Number of genes covered by RRBS analysis = 1161* Hypomethylated DMRs = 1884 (82%) Hypermethylated DMRs = 413 (18%)	*Number of genes covered by RRBS analysis = 163* Hypomethylated DMRs = 274 (81%) Hypermethylated DMRs = 66 (19%)
Promoter Region (-5kb to 1kb)	*Number of genes covered by RRBS analysis = 686* Hypomethylated DMRs = 784 (81%) Hypermethylated DMRs = 181 (19%)	*Number of genes covered by RRBS analysis = 77* Hypomethylated DMRs = 92(82%) Hypermethylated DMRs = 20 (18%)
Putative Enhancers (H3k4me2)	*Number of genes covered by RRBS analysis = 837* Hypomethylated DMRs = 1180 (83%) Hypermethylated DMRs = 242 (17%)	*Number of genes covered by RRBS analysis = 117* Hypomethylated DMRs = 175 (81%) Hypermethylated DMRs = 40 (19%)

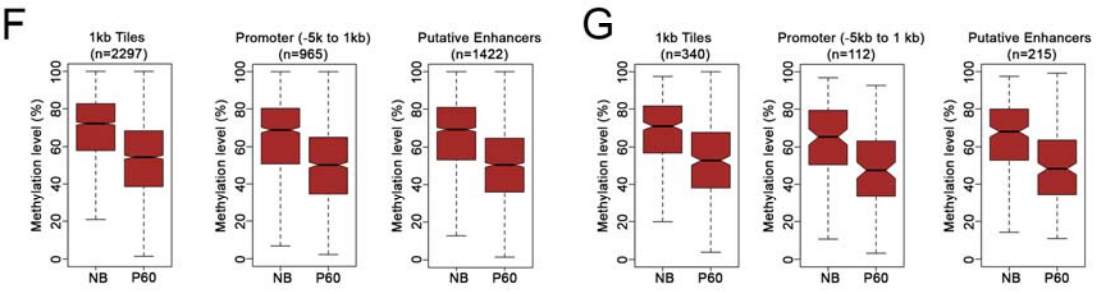

Figure S2, related to Figure 2

Figure S2: Differentiation-specific genes are hypomethylated at gene-regulatory regions, related to Figure 2

(**A**) Violin plot showing differential gene expression between NB and P60 nerves, with about an equal number of upregulated and downregulated genes. (**B**) Boxplot showing methylation levels of all tiling regions associated with up-regulated or down-regulated genes. (**C,D)** Scatterplot of percentage DNA methylation levels of 1-kb tiles in NB and P60 nerves, mapped to (**C**) promoter regions (-5kb to 1 kb surrounding Ensembl-annotated TSS) or (**D**) putative enhancers (H3K4me1 peaks). Hypomethylated regions are shown in *blue* and hypermethylated regions are shown in *red* ($q<0.05$, methylation difference of at least 10%). Selected genes with important functions in Schwann cell myelination are highlighted. (**E**) Table showing the number of hypomethylated or hypermethylated DMRs ($q<0.05$, methylation difference of 20%) for different genomic regions (1 kb tiles, promoter region and putative enhancers) associated with all upregulated genes or upregulated genes specifically in lipid metabolism category in P60 nerves compared to NB nerves, covered by RRBS analysis. On average, for all categories analyzed, there was a 4-fold higher of hypomethylated DMRs than hypermethylated DMRs associated with the covered genes. Please note that for some genes, several DMRs were found to be associated with them. (**F, G)** Boxplots showing percentage methylation levels of all differentially-methylated genomic regions for (**F**) all upregulated genes (**G**) upregulated genes specifically in lipid metabolism, covered by RRBS analysis from (**E**). Number of genomic sites (*n*) is indicated.

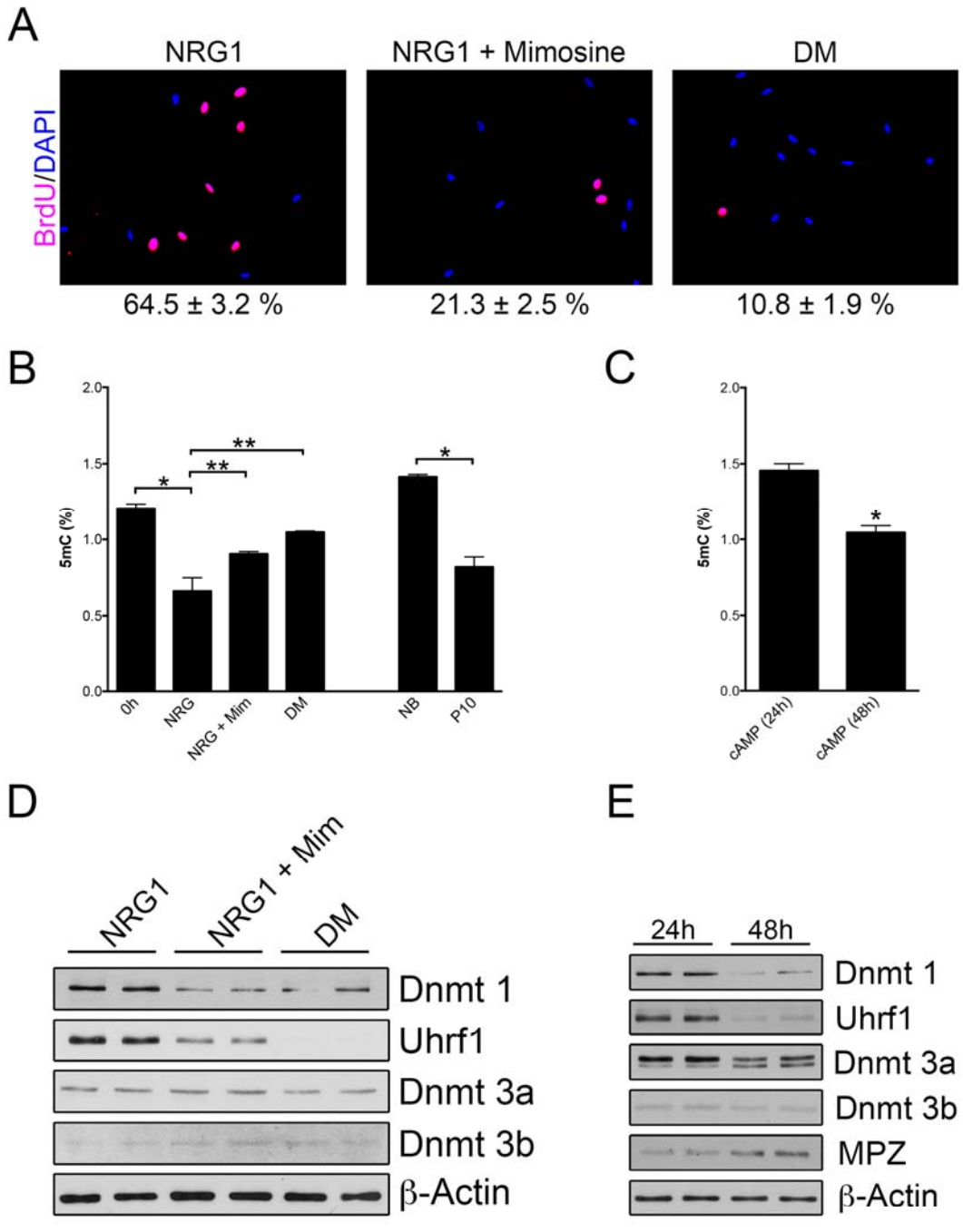

Figure S3, related to Figure 3

Figure S3: Regulation of methylation dynamics during Schwann cell development, related to Figure 3

(**A**) Immunocytochemistry showing NRG1-induced proliferation in Schwann cell cultures, as seen by BrdU incorporation ($BrdU^+$ cells, red; DAPI_nuclei, blue). Proliferation is significantly blocked by treatment with 1mM mimosine (blocks cell cycle at the G1 to S transition), or switching to medium without NRG1 (DM). Percentage $BrdU^+$ cells of each condition is shown below the pictures. (**B**) Measurement of global DNA methylation level by ELISA with an antibody directed at 5-methylcytosine. NRG1 treatment of Schwann cell cultures for 16h induces a significant decrease in global DNA methylation. This demethylation was reduced by cell cycle block with mimosine or by culture in DM. As a comparison, global DNA demethylation is shown in P10 nerves compared to NB nerves. *, ** $p<0.05$. Data is mean ± sem. n=3. (**C**) Culture of Schwann cells in myelinogenic conditions (48h cAMP treatment compared to 24h treatment) leads to Schwann cell DNA demethylation. *,$p<0.05$. Data is mean ± sem. n=3. (**D**) Western blot analysis showing reduced expression of DNA methyltransferases Dnmt1 and Uhrf1 in Schwann cell cultures after cell cycle block. This is similar to *in vivo* Schwann cell differentiation when proliferative stages (NB) are compared to quiescent stages (P10 and P60 nerves) (Figure 3D). β-Actin is used as a loading control. (**E**) Western blot analysis showing reduced expression of DNA methyltransferases in Schwann cell cultures under myelinogenic conditions. This is similar to *in vivo* terminal differentiation of myelinating Schwann cells (P60 nerves compared to P10 nerves) (Figure 3D). β-Actin is used as a

loading control. MPZ shows increased levels in cultures treated for 48h with cAMP compared to cultures treated for 24h.

A

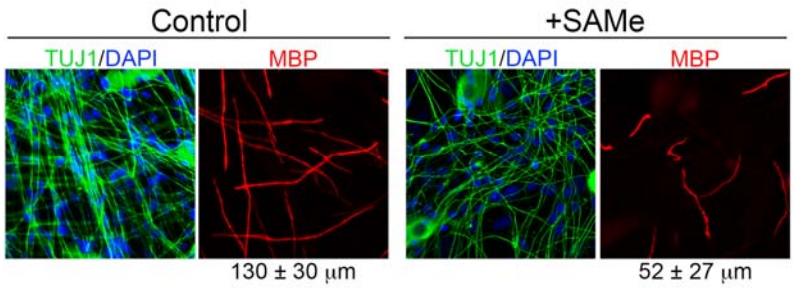

B

Sample	n	Input	CpGs (1X)	Unique (1X)	Mean Coverage (1X)	r
Control	2	1X 10^6 cells per replicate	53,670,997	1,609,806	33.1	0.87
SAMe	2	1X 10^6 cells per replicate	37,875,581	1,369,773	26.5	0.85

C

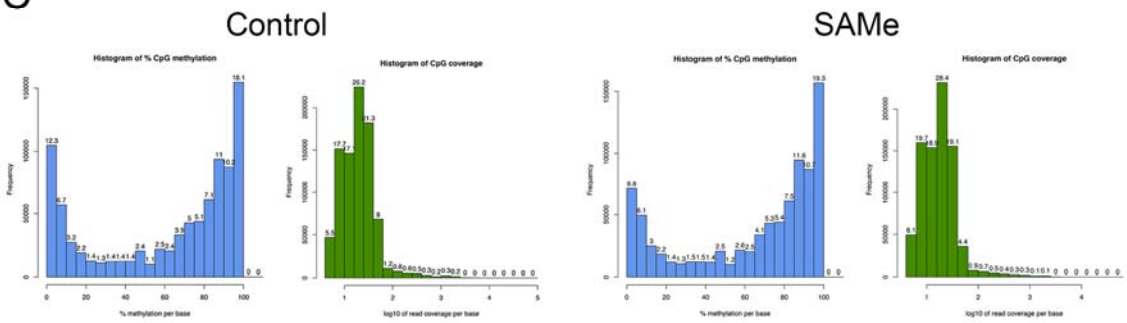

D

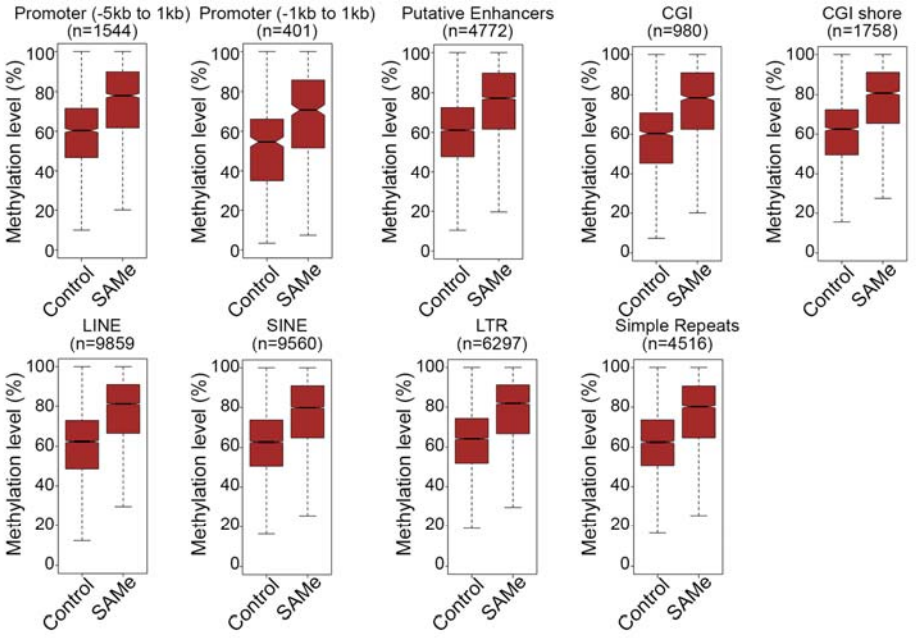

Figure S4, related to Figure 4

Figure S4: Methylation dynamics in control and SAMe-treated Schwann cell cultures, related to Figure 4

(**A**) High magnification pictures of Schwann cell-DRG co-cultures with or without SAMe supplementation (Figure 4E). MBP^+ internodes in control cultures were significantly longer than in SAMe-treated cultures. Average length of internodes in control cultures was 130 ± 30 μm, whereas in SAMe-treated cultures was 52 ± 27 μm. (**B, C**) Basic RRBS statistics of control and SAMe-treated Schwann cell cultures. (**B**) Table of CpG coverage captured by RRBS showing the number of replicates (*n*), input (number of cells used per replicate), numbers of total and unique CpGs covered at least once (1X), mean coverage and mean Pearson´s correlation (*r*) between the replicates for each culture condition. (**C**) Distribution histograms of CpG methylation levels (*left panels*) and CpG coverage (*right panels*) for control and SAMe-treated Schwann cell cultures. A representative replicate for each culture condition is shown. (**D**) Boxplots showing increased methylation levels of all differentially-methylated 1-kb tiling regions mapped to different genomic regions ($q<0.05$, methylation difference of 20%) in SAMe-treated cultures compared to control cultures. Number of genomic sites (*n*) is indicated.

A

Sample	n	Input	CpGs (1X)	Unique (1X)	Mean Coverage (1X)	r
Gnmt$^{+/+}$	2	2-3 per replicate	39538770	1291559	29.9	0.86
Gnmt$^{-/-}$	2	2-3 per replicate	10521868	637517	16.5	0.81

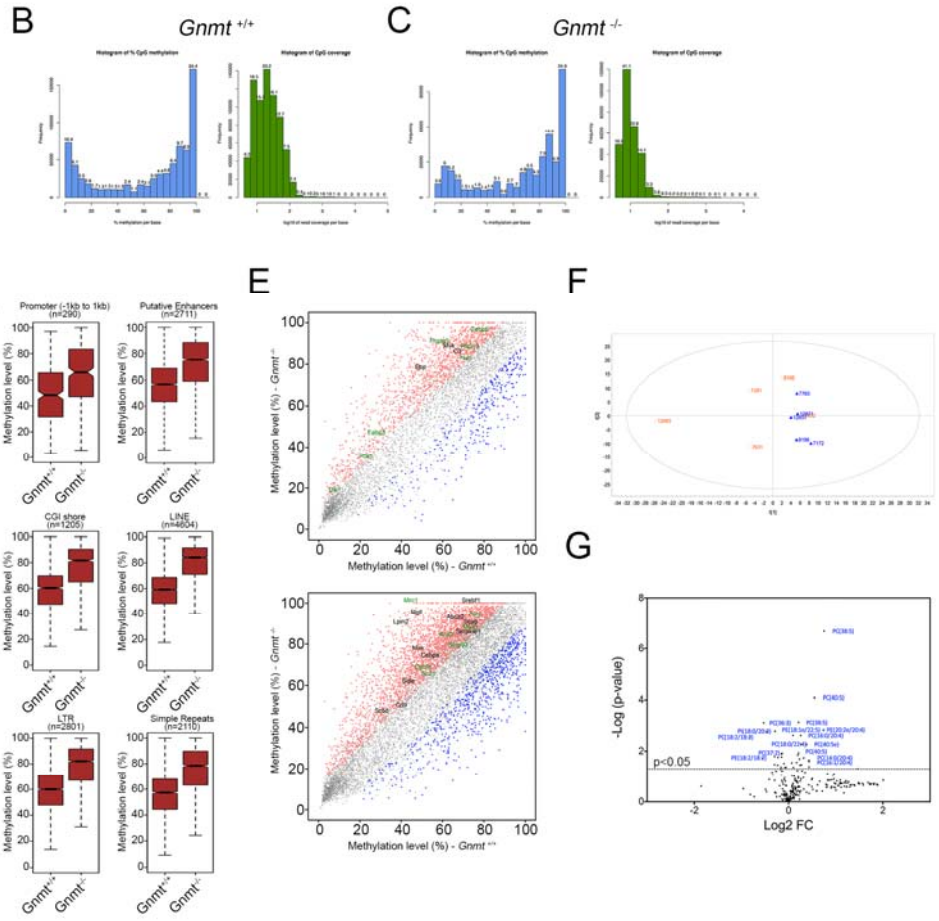

Figure S5, related to Figure 6

Figure S5: Methylation dynamics in *Gnmt*$^{+/+}$ and *Gnmt*$^{-/-}$ mice, related to Figure 6

(**A-C**) Basic RRBS statistics of *Gnmt*$^{+/+}$ and *Gnmt*$^{-/-}$ samples. (**A**) Table of CpG coverage captured by RRBS showing the number of replicates (*n*), input (number of mice used for sciatic nerve isolation), numbers of total and unique CpGs covered at least once (1X), mean coverage and mean Pearson´s correlation (*r*) between the replicates for each genotype. (**B,C**) Distribution histograms of CpG methylation levels (*left panels*) and CpG coverage (*right panels*) for (**B**) *Gnmt*$^{+/+}$ and (**C**) *Gnmt*$^{-/-}$ mice. A representative replicate of each genotype is shown. (**D**) Boxplots showing methylation levels of differentially-methylated 1-kb tiling regions (q<0.05, methylation difference of 20%), annotated to gene-regulatory regions and repeat elements. Number of genomic sites (*n*) is indicated. (**E**) Scatterplot of DNA methylation of 1-kb tiles in *Gnmt*$^{+/+}$ and *Gnmt*$^{-/-}$ nerves, annotated to promoter regions (-5kb to 1 kb surrounding Ensembl-annotated TSS)(*upper* panel) or putative enhancers (H3K4me1 peaks) (*bottom* panel). Hypomethylated regions are shown in *blue* and hypermethylated regions are shown in *red* (q<0.05, methylation difference of at least 10%). Selected hypermethylated genes are highlighted (genes which are downregulated are shown in *green*). (**F**, **G**) Metabolomic profiling shows significant differences between *Gnmt*$^{+/+}$and *Gnmt*$^{-/-}$ mice. (**F**) Principal component analysis (PCA) of all metabolites analyzed showed clear sample segregation according to mice genotype with wildtype samples located on the right side (*blue triangles*) and knockouts on the left side (*orange triangles*). (**G**) Violin plot showing several lipid species with significant

changes in expression in *Gnmt*$^{-/-}$ mice compared to *Gnmt*$^{+/+}$ mice. Threshold $p<0.05$ value is indicated with dotted lines (n=5; *Student´s t-test)*.

A

Sample	n	Input	CpGs (1X)	Unique (1X)	Mean Coverage (1X)	r
sh Control	2	1X 10^6 cells per replicate	57,485,918	1,744,528	32.2	0.86
sh GNMT	2	1X 10^6 cells per replicate	37,969,259	1,290,149	29.5	0.86
sh GNMT (MDM)	2	1X 10^6 cells per replicate	62,238,635	1,921,949	31.6	0.87

B

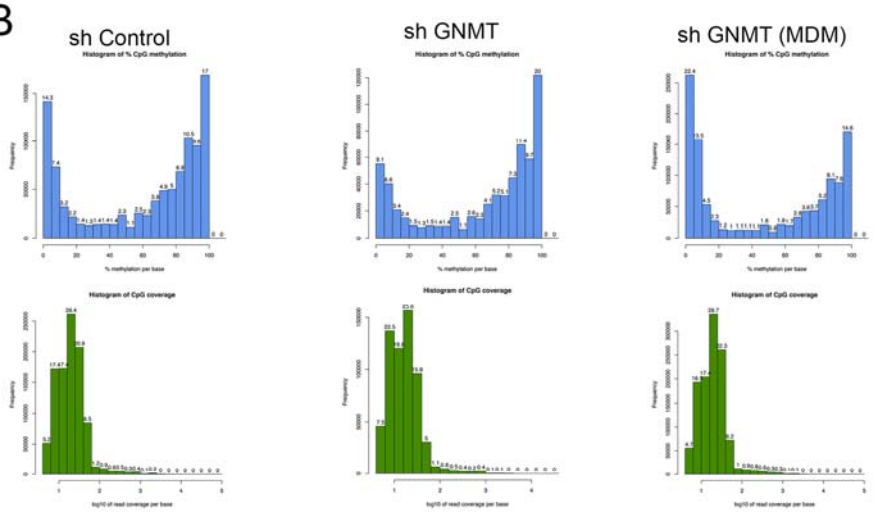

C

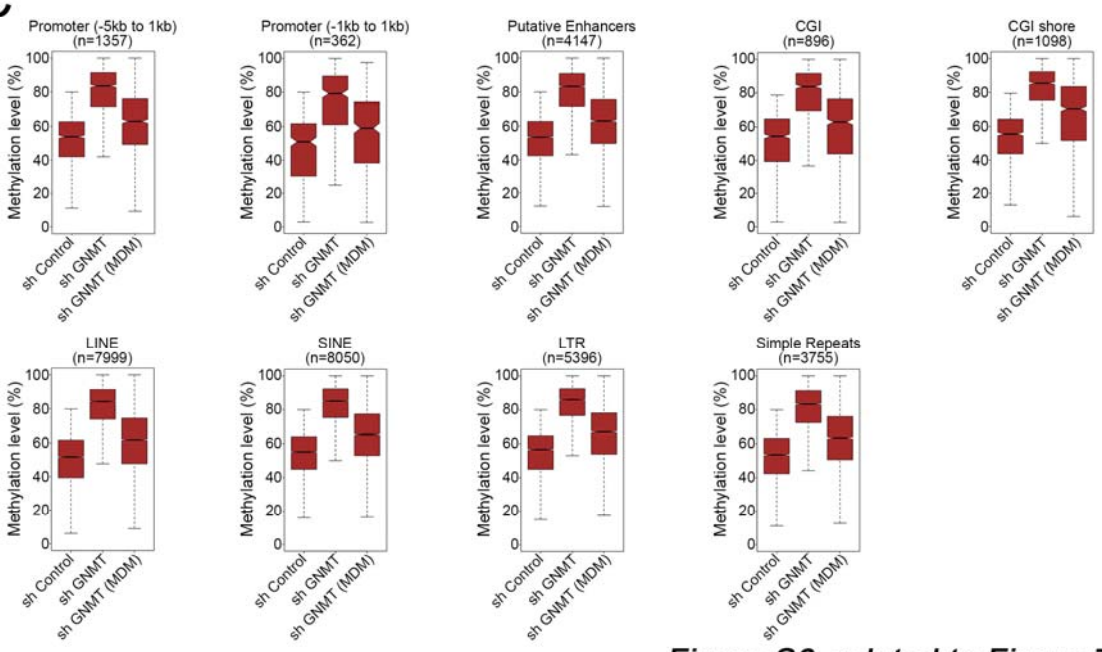

Figure S6, related to Figure 7

Figure S6: Methylation dynamics in *sh GNMT*-silenced Schwann cell cultures, related to Figure 7

(**A**,**B**) Basic RRBS statistics in sh Control-infected Schwann cell cultures (sh Control), sh GNMT-silenced Schwann cell cultures (sh GNMT) and sh GNMT-silenced Schwann cell cultures cultured in low methionine medium (sh GNMT_MDM). (**A**) Table of CpG coverage captured by RRBS showing the number of replicates (*n*), input (number of cells used per replicate), numbers of total and unique CpGs covered at least once (1X), mean coverage and mean Pearson´s correlation (*r*) between the replicates for each cell type. (**B**) Distribution histograms of CpG methylation levels (*upper panels*) and CpG coverage (*bottom panels*) for each cell type. A representative replicate for each culture condition is shown. (**C**) Boxplots showing increased methylation levels of all differentially-methylated 1-kb tiling regions mapped to different genomic regions (q<0.05, methylation difference of 20%) in *GNMT*-silenced cells cultures (sh GNMT) compared to control cultures (sh Control). This effect is abolished when sh GNMT cells were cultured in low methionine medium (sh GNMT_MDM). Number of genomic sites (*n*) is indicated.

A

Sample	n	Input	CpGs (1X)	Unique (1X)	Mean Coverage (1X)	r
db/+	2	2-3 per replicate	15325031	797675	18.6	0.81
db/db	2	2-3 per replicate	28487470	1271488	22.4	0.84

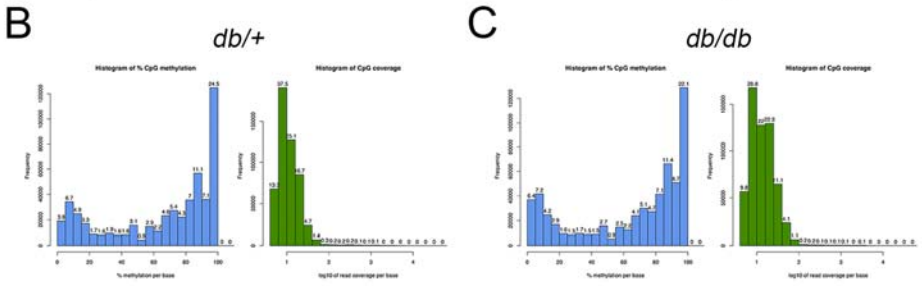

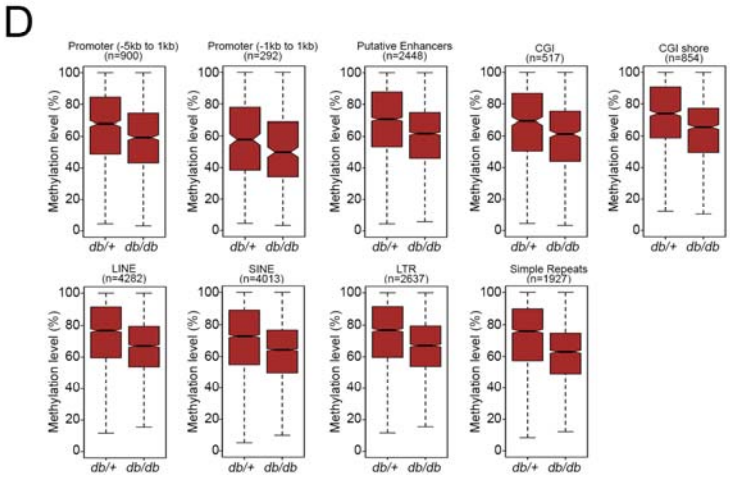

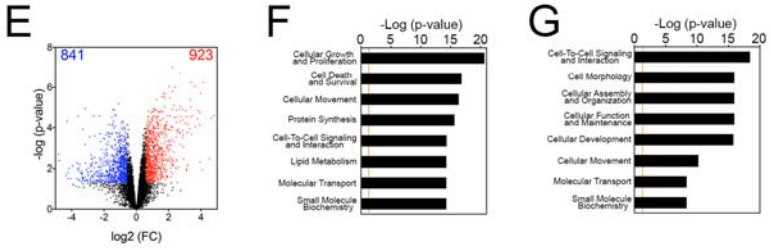

H

	4 weeks		8 weeks		16 weeks	
	db/+	db/db	db/+	db/db	db/+	db/db
Weight (g)	21.8 ± 0.2	22.1 ± 0.4	24.6 ± 0.4	**42.3 ± 2.2***	29.1 ± 0.9	**54.9 ± 1.7***
Thermal latency	4.7 ± 1.5	4.8 ± 1.2	4.5 ± 1.0	**5.7 ± 0.3***	4.2 ± 1.2	**6.1 ± 0.9***
Methionine	239.5 ± 16.2	246.2 ± 16.3	155.1 ± 8.8	156.2 ± 9.7	111.6 ± 10.1	121.6 ± 9.8
SAMe	3.6 ± 0.3	3.6 ± 0.2	3.5 ± 0.2	**2.7 ± 0.2***	3.3 ± 0.1	**1.9 ± 0.0***
SAH	6.1 ± 1.4	6.8 ± 0.9	3.6 ± 0.6	**6.8 ± 0.8***	2.7 ± 0.5	3.9 ± 0.3
SAMe/SAH ratio	0.8 ± 0.2	0.6 ± 0.1	1.1 ± 0.2	**0.4 ± 0.0***	1.4 ± 0.2	**0.5 ± 0.0***

Figure S7, related to Figure 8

Figure S7: Methylation dynamics in *db/+* and *db/db* mice, related to Figure 8

(A-C) Basic RRBS statistics of *db/+* and *db/db* samples. **(A**) Table of CpG coverage captured by RRBS showing the number of replicates (*n*), input (number of mice used for sciatic nerve isolation) at each stage, numbers of total and unique CpGs covered at least once (1X), mean coverage and mean Pearson´s correlation (*r*) between the replicates. **(B,C)** Distribution histograms of CpG methylation levels (*left panels*) and CpG coverage (*right panels*) for **(B)** *db/+* and **(C)** *db/db* mice. A representative replicate of each genotype analyzed is shown. **(D)** Boxplots showing methylation levels of differentially-methylated 1-kb tiling regions (q<0.05, methylation difference of 20%), annotated to gene-regulatory regions and repeat elements. Number of genomic sites (*n*) is indicated. **(E)** Violin plot showing differential gene expression between *db/+* and *db/db* nerves, with about an equal number of upregulated (*red*) and downregulated (*blue*) genes using published dataset (Pande et al., 2011). **(F, G)** GO analysis showing top Molecular and Cellular Function categories enriched in **(F)** up-regulated genes and **(G**) down-regulated genes in *db/db* mice. **(H**) Table showing phenotyping parameters and levels of the metabolites methionine, SAMe and SAH (pmol mg^{-1} of tissue), and the SAMe/SAH ratio in *db/+* and *db/db* mice at different ages. At the onset of diabetes (4 weeks), peripheral neuropathy has not yet developed, and we find no significant differences in metabolite levels between *db/+* and *db/db* mice. Interestingly, at 8 weeks when diabetic neuropathy has already developed, as determined by thermal latency (tail flick test) here and in line with other studies, including nerve conduction velocity and intraepidermal fiber

measurements(Sullivan et al., 2008), we found significant differences in SAMe and SAH levels, which resulted in a decreased SAMe/SAH ratio in *db/db* mice compared to *db/+* mice. A similar result was obtained in 16 weeks old mice. Data is mean ± sem, n=5, *Student´s t-test*. * $p<0.05$.

SUPPLEMENTAL TABLE LEGENDS

Table S1, related to Figure 1

Methylation level and coverage (number of reads) of all 1-kb tiles with sufficient valid sequencing read (≥5) in individual replicates of NB and P60 nerves. Methylation difference and *q*-values are also shown.

Table S2, related to Figure 2

Worksheet 1 and 2: Gene expression changes from micro-array experiments during different stages of Schwann cell myelination. The list shows the fold-change and adjusted *p*-value (*Experimental Procedures*) in the comparison P60 *vs*. NB (sheet 1) and P10 *vs*. NB (sheet 2). "DD" represents significantly downregulated genes, "UU" represents significantly upregulated genes, and "-" represents genes not significantly changed.

Worksheet 3: Full results of GO analysis using Ingenuity IPA for (i) upregulated genes, (ii) upregulated genes that are hypomethylated in 1-kb tiles, and (iii) upregulated genes that are hypomethylated in promoter and/or putative enhancer regions in the comparison of P60 nerves to NB nerves. Enrichment *p*-value and molecules present for each category are shown.

Worksheet 4: Full list of enrichment of TF binding motifs in hypomethylated regions for P60 vs NB analysis. Enrichment values are shown as *Z*-score.

Table S3, related to Figure 3

Methylation level and coverage of all 1-kb tiles with sufficient valid sequencing read (≥5) in individual replicates in pair-wise comparison of (*Sheet 1*) P10 vs

NB and (*Sheet 2*) P60 vs P10 nerves. Methylation difference and *q*-values are also shown.

Table S4, related to Figure 4

Methylation level and coverage (number of reads) of all 1-kb tiles with sufficient valid sequencing read (≥5) in individual replicates of Control and SAMe-treated Schwann cell cultures. Methylation difference and *q*-values are also shown.

Table S5, related to Figure 5

Worksheet 1: Gene expression changes from micro-array experiments of *Gnmt*$^{+/+}$ and *Gnmt*$^{-/-}$ nerves. The list shows the fold-change in *Gnmt*$^{-/-}$ *mice* relative to *Gnmt*$^{+/+}$ mice and adjusted *p*-value (*Methods*). "DD" represents significantly downregulated genes, "UU" represents significantly upregulated genes, and "-" represents genes not significantly changed.

Worksheet 2: Full results of GO analysis using Ingenuity IPA for (i) downregulated genes, (ii) downregulated genes that are hypermethylated in 1-kb tiles, and (iii) downregulated genes that are hypermethylated in promoter and/or putative enhancer regions in *Gnmt*$^{-/-}$ relative to *Gnmt*$^{+/+}$ mice. Enrichment *p*-values and molecules present for each category are shown.

Table S6, related to Figure 6

Worksheet 1: Methylation level and coverage of all 1-kb tiles with sufficient valid sequencing read (≥5) in individual replicates of *Gnmt*$^{+/+}$ and *Gnmt*$^{-/-}$ nerves. Methylation difference and *q*-values are also shown.

Worksheet 2: Metabolomic profiling results in *Gnmt*$^{+/+}$ and *Gnmt*$^{-/-}$ nerves, showing measurements for all metabolites.

Table S7, related to Figure 7

Methylation level and coverage (number of reads) of all 1-kb tiles with sufficient valid sequencing read (≥5) in individual replicates of sh Control-infected Schwann cell cultures (sh Control), sh GNMT-silenced Schwann cell cultures (sh GNMT) and sh GNMT-silenced Schwann cell cultures cultured in low methionine medium (sh GNMT_MDM). Methylation difference and *q*-values are also shown for the following comparisons (1) sh GNMT_v_sh Control (2) sh GNMT (MDM) _v_sh Control, and (3) sh GNMT (MDM) _v_sh GNMT.

Table S8, related to Figure 8

Worksheet 1: Methylation level and coverage of all 1-kb tiles with sufficient valid sequencing read (≥5) in individual replicates of *db/+* and *db/db* nerves. Methylation difference and *q*-values are also shown.

Worksheet 2 and 3: Full results of GO analysis using Ingenuity IPA for the comparison between *db/db* mice and *db/+* mice. *Sheet 2* shows (i) downregulated genes, (ii) downregulated genes that are hypermethylated in 1-kb tiles, and (iii) downregulated genes that are hypermethylated in promoter and/or putative enhancer regions. *Sheet 3* shows (i) upregulated genes, (ii) upregulated genes that are hypomethylated in 1-kb tiles, and (iii) upregulated genes that are hypomethylated in promoter and/or putative enhancer regions. Enrichment *p*-values and molecules present for each category are shown.

SUPPLEMENTAL EXPERIMENTAL PROCEDURES

Animals. Mice and rats were housed at the Animal unit at CIC bioGUNE (AAALAC-accredited facility). All procedures were approved by the institutional committee on animal use. Sciatic nerves were isolated from C57 BL6/J mice at newborn (NB), post-natal day 10 (P10) and P60 ages. *Gnmt*$^{-/-}$ mice were described previously(Martinez-Chantar et al., 2008) and nerves isolated at P90. *Db/db* mice, as described previously(Pande et al., 2011), were purchased from Jackson Laboratories and nerves extracted at different ages. Nerves from mice of either sex were used. Immediately after isolation, nerves were desheathed and flash-frozen in liquid nitrogen.

Reduced Representation Bisulfite sequencing. Preparation of RRBS libraries was adapted from published protocols(Gu et al., 2011), and libraries were sequenced by the CIC bioGUNE Genome Analysis Platform on a HiScanSQ platform (Illumina Inc.). Data processing reads were created by CASAVA 1.8.2. Reads were filtered from the adapter sequences and their quality scored using trim_galore software (http://www.bioinformatics.babraham.ac.uk/projects/trim_galore/). Only those with at least 20 phred quality score were retained. Reads were aligned to the Mouse Genome Build 37 (mm9) using the BSMAP (http://rrbsmap.computational-epigenetics.org/) using the following parameters -s 12 -D C-CGG. In order to call methylation score for a base position, we required that read bases aligning to that position had at least 5X coverage. We used the MethylKit R package to compute methylation ratios and differential methylation analysis(Akalin et al., 2012). For all RRBS

experiments, a minimum of two independent biological replicate pools was used.

The DNA methylation levels of single CpGs were estimated as the ratio of cytosines observed among the bisulfite sequencing reads divided by the sum of observed cytosines (indicative of methylated DNA) and thymines (indicative of unmethylated DNA). Average DNA methylation levels were calculated for 1-kb tiling regions throughout the genome as the coverage-weighted means of the DNA methylation levels of individual CpGs. Only regions with at least two CpGs and at least 5 independent DNA methylation measurements per CpG were retained. These 1-kb tiles were used for all analyses, including annotations to genomic regions.

LINE, LTR, Simple Repeats and SINE annotations were downloaded from the UCSC browser RepeatMasker tracks. Promoter regions (-5kb to 1kb from TSS), promoter regions centered (-1kb to 1kb from TSS), CpG Islands, CpG Island shores and refseq genes annotations were downloaded from the UCSC genome browser. Annotations for putative enhancers as defined by presence of H3K4me1 marks were obtained from ENCODE/LICR at UCSC genome browser(Shen et al., 2012). H3K4me1 marks were used for 6 different mouse tissues (Bone Marrow, Cerebellum, Cortex, Heart, Kidney and Liver) since DMRs analyzed showed significant enrichment for them with EpiExplorer.

Gene Expression microarray analysis. Total RNA was isolated from different sets of nerves using standard techniques and cRNA libraries hybridized to the MOUSEWG-6 V2 BeadChips (Illumina Inc.). Data were

processed as described(Iruarrizaga-Lejarreta et al., 2012). Adjustment of *p*-values was done by the determination of false discovery rates (FDR) using Benjamini-Hochberg procedure. For developmental studies, 3 biological replicates of NB, P10 and P60 developmental stages were used, whereas for GNMT mice, 2 biological replicates of each genotype were used. The number of mice used for each replicate was on average: NB (20), P10 (10) and P60 (5), *Gnmt*$^{+/+}$ mice (5) and *Gnmt*$^{-/-}$ mice (5).

Bioinformatic Analyses. Identification of differentially methylated regions was performed by Methylkit, and a tile or genomic regions were considered to be differentially methylated if it both had a methylation difference of ≥20% between two stages and was significant in a two-sample *t*-test with unequal variance after correction for multiple hypothesis testing (FDR or *q*-value <0.05) using the Benjamini–Hochberg method. Chromosome ideograms (e.g. Figure 1E) were done with Methylkit. Classification of DMRs into enriched genomic regions (e.g. Figure 1G) was done with EpiExplorer software(Halachev et al., 2012). Association of DMRs to gene regions (e.g. Figure 1F) was done with GREAT software (McLean et al., 2010).

For comparison of DNA methylation and gene expression changes, we used previously described criteria(Bock et al., 2012). Thus, for DNA methylation, we used methylation differences of at least 10% (q<0.05) and for gene expression changes, we required a minimum absolute difference of $\log_2(1.5)$ (q<0.05). For microarray experiments, when several probes mapped to the same gene showed statistically significant differences, we used the probe with the most significant *q*-value. Similarly for DNA methylation

mRNA	Forward (5'-3')	Reverse (5'-3')

measurements, we frequently detected that several tiles were mapped to the same gene, promoter region (-5kb to 1kb from TSS) or enhancer. In this case, also, the methylation level of the tile showing most significant statistical difference (*q*-value) was taken to represent the methylation level of that region. Since DNA methylation at promoter regions and enhancers have been more consistently linked to regulation of gene expression(Bock et al., 2012; Jones, 2012), we combined these regions to check for association with gene expression changes, and are referred to as “gene-regulatory regions” in the text.

Biological functional analysis was performed using Ingenuity Pathway Analysis software (Ingenuity Systems). Fisher’s exact test was performed with the *p-value* value threshold of 0.05 to identify molecular functional categories with statistical significance.

RNA isolation and quantitative PCR (qPCR). RNA was isolated with Trizol (Invitrogen). qPCRs were performed using BioRad iCycler thermocycler. Ct values were normalized to the housekeeping expression (*GAPDH*). For all qPCR analyzes performed, 3 biological replicates were used. The number of mice used for each replicate was on average: NB (20), P10 (10) and P60 (5), *db/+* mice (4) and *db/db* mice (4). Primer sequences used:

Dnmt1	CTAGTTCCGTGGCTACGAGG	AGTTCCCCTCTTCCGACTCT
Dnmt3a.1	GCGGGAGGATGATCGAAAGG	GGGGTGTCACTGCTTTCCAC
Dnmt3a.2	GGCTCACACCTGAGCTGTACT	TGGTTCTCTTCCACAGCATTCA
Dnmt3b	CCCATCCATAGTGCCTTGGG	AATGCACTCCTCATACCCGC
Dnmt3l	AGGAACGCTGAAGTACGTGG	GAGCCGTACACCAGGTCAAA
Uhrf1	GCTGGATTGTGTCATTGAGG	GAACCCCAACTGCAGAGACT
Gadd45a	CTGCAGAGCAGAAGACCGAA	GGGTCTACGTTGAGCAGCTT
Gadd45b	TGTGCATAAGTCAGCGGAGG	ATGTGCTGTAGCTGCGAAGT
Gadd45g	CCCTCCGCACTCTTTTGGAT	CAGCAGAAGTTCGTGCAGTG
AID	AGTCACGCTGGAGACCGATA	GCAGAGGTAGGTCTCATGCC
Apobec1	GACCTTCAGCTAACCTCACACA	CTCTGTCTCTGGACGCCTTC
Tdg	CCCCACAAGATCCCAGACAC	CGGGGAAACTGAGCACATCT
Mbd4	AGGATGGCTCTGAAATGCCC	TACTTGTGTCCGTGGGATGC
Tet1.1	AACCGGGTGGATCATTCCAG	ACTGGAGCCATCTGCTTGTAA
Tet1.2	GCTCCAAACTACCCCTTACATGA	TCGACAGTCTCCAGCAACTTC
Tet2	TGGCTGCCCTGTAGGATTTG	CCGTAGCGGAACAGGAACAA
Tet3	GCATGTACTTCAACGGCTGC	AGTGGCCAGATCCTGAAAGC
Mat2a	TGAAGGTGTGCATCAAGGAC	CGTTCCTCTTCACTTCCGAG
Gnmt	ACCAGTATGCAGATGGGGAG	CCAATTGTCAAAGGATGGCT
Sahh	CCTGGCATCTCATTCTCAGC	CGCCAGCATGTCTGATAAAC
Pemt	AGTTCTCTGCTCCCATCTCG	GGTTACATGGACCCCACAGA
Bhmt	GAACTCCCGATGAAGCTGAC	CTTTGCACTGGAAAAGAGGG
Mtr	CATCCAAGAGTGTGGTGGTG	ATAAACGTGGGCTTCACTGG
Cbs	TGTTGATTCTGACCATAGGGG	CGGACTCCCCACATTATCAC
Cth	TGTTAAGGCCTTCCTCAAAA	GTCCTTCTCAGGCACAGAGG
Gapdh	TGCACCACCAACTGCTTAG	GGATGCAGGGATGATGTTC

Protein isolation and western blotting. Isolation and western blotting of total proteins from cells and nerves were done as described(Iruarrizaga-Lejarreta et al., 2012). The following antibodies were used: Gapdh (Abcam, ab8245), Dnmt1 (Abcam, ab13537) and Dnmt3a (Abcam, ab13888), β-actin (Sigma, A5441), Egr2 (Covance, PRB-236P) and TuJ1 (Covance, MRB-

435P), MPZ (gift from JJ Archelos), Periaxin (gift from P. Brophy), MBP (Covance, SMI-99P), GNMT (gift from C. Wagner), Dnmt3b (Abcam, ab2851) Dnmt3b (Imgenex, IMG-184A) and Uhrf1 (Santa Cruz Biotechnology, sc-373750). For WB of total nerve extracts, each figure shows the pattern of expression of 2 independent biological replicates for each group. The number of mice used for each replicate was on average: NB (10), P10 (3) and P60 (3), *Gnmt*$^{+/+}$ mice (3), *Gnmt*$^{-/-}$ mice (3), *db/+* mice (3) and *db/db* mice (3). For WB of cultured cells, the figures show the pattern of expression of 2 independent technical replicates for each group. These experiments were performed 3 times.

Primary Schwann cell culture & cAMP myelination assay. Schwann cells were isolated from P5 sciatic nerves of Wistar rats or P5-P8 sciatic nerves from C57 BL6/J mice, and purified and cultured as described before(Iruarrizaga-Lejarreta et al., 2012), except that horse serum was used instead of FBS for mouse Schwann cells. Only the first 5 passages were used. For myelination assays, a cAMP analogue, dibutryl cAMP (10^{-3} M), was added to cultures for 2 days. For mouse Schwann cells, the medium was also supplemented with NRG1 (10 ng ml^{-1}).

Organotypic rat neuron-Schwann cell co-cultures. Dorsal root ganglia (DRG) were isolated from embryonic day 15 (E15) Wistar embryos, and seeded onto PDL-laminin coated coverslips and allowed to attach for 24 hrs. DRG were cultured for 2 weeks to allow the growth of neurons and their association with endogenous Schwann cells. The cultures were treated with

50 mg ml^{-1} ascorbic acid for about 10 days to allow myelination. Cultures were fixed and antibodies to MBP were used to label myelin sheaths. For quantification, number of MBP^+ myelin sheaths per field (40X objective) was counted in 10 separate randomly chosen fields per coverslip. 2 independent experiments were carried out, each with 3 coverslips per condition. Thus, a total of 6 coverslips was counted per condition.

Viral infection. Cells were treated with control lentiviral particles (pLKO.1) or short-hairpin lentiviral particles against GNMT (Sigma Mission clone: TRCN0000097601) in the presence of hexadimethrine bromide (8 μg ml^{-1}). After 24h transduction, the cells were selected using puromycin (1.25 μg ml^{-1}).

S-Adenosylmethionine treatment. SAMe, in the stable form of sulfate-p-toluensulfonate (Samyr) was obtained from Abbott or Sigma, and used freshly prepared at a concentration of 2mM.

Global DNA methylation analysis

Global DNA methylation was quantified by specifically measuring levels of 5-methylcytosine (5-mC) in an ELISA-like microplate-based format using the MethylFlash™ Methylated DNA Quantification Kit (Epigentek). Purified gDNA (100 ng) was used.

For studies of proliferation on global DNA methylation, Schwann cells were isolated from NB Wistar rat pups, and plated onto laminin-coated dishes. After 3-4 h following attachment of cells to surface, cells were treated for 16h with NRG1 (20 ng/ml)(R&D Systems), or 1 mM mimosine (Sigma) or switched to

Defined Medium (DM)(Iruarrizaga-Lejarreta et al., 2012). Sister cultures were extracted after the initial attachment, and represent 0h time-point of the experiment.

For studies of myelination on global DNA methylation, as described above, serum-purified Schwann cells were treated with cAMP for 24h and 48h.

Assessment of neuropathy (Thermal latency)

The tail flick test was done as a measure of thermal latency, essentially as described previously(Lee et al., 1990). In brief, the tail of each mouse was placed in 50^0 C water, and the latency to flick was recorded. For each mouse, the thermal latency was recorded three times, with a 30 min interval between each measurement, and then averaged. For each group, thermal latency was measured in at least 5 mice.

In vitro RRBS analysis. (1) Purified mouse Schwann cells cultured under myelinogenic conditions were either treated or untreated for 2 days with SAMe, and then genomic DNA extracted for RRBS analysis. (2) Puromycin-selected shControl and shGNMT-silenced cells were switched to myelinogenic conditions for 2 days, and then genomic DNA extracted. For MDM treatment, shGNMT cells were switched to myelinogenic conditions for 2 days (medium containing 10 μm methionine) and then genomic DNA extracted.

Electron Microscopy and morphometric analyses. Processing of nerve samples was carried out as described(Woodhoo et al., 2009) and sections

were viewed in a Jeol 1010 transmission electron microscope (TEM). Morphometric analyses, calculations of G-ratio and axon diameter distribution in adult nerves are described(Woodhoo et al., 2009). G-ratio is the ratio of the inner axonal diameter to the total outer diameter and is a highly reliable parameter for assessing myelination. For these analyzes, at least 50 myelinated axons were counted in each of 5 different sets of nerves obtained from different mice of either genotype. For early myelination studies, images of whole P5 nerves were acquired under TEM and analyzed using NIH Image J. The number of myelinating Schwann cells was counted in each nerve and expressed as a percentage of Schwann cells in a 1:1 relationship with axons (myelinating Schwann cells and pro-myelin Schwann cells). The myelin thickness of about 200 Schwann cells in each nerve was determined and the proportion of Schwann cells within a particular myelin thickness range calculated. These analyzes were performed in 5 different sets of nerves obtained from different mice of either genotype.

Metabolite measurements and profiling. For quantitative metabolite measurements (SAMe, SAH or methionine), several sets of nerves or Schwann cell cultures were pooled together and analysis performed(Martinez-Chantar et al., 2008) at CIC bioGUNE´s Metabolomics Platform. For these analyzes, 5 independent biological replicates for each group were used, with each replicate consisting of several sets of nerves obtained from different mice or $2x10^6$ cells per culture condition. The number of mice used for each replicate was on average: P10 (20) and P60 (10), *Gnmt*$^{+/+}$ mice (5), *Gnmt*$^{-/-}$ mice (5), *db/+* mice (5) and *db/db* mice (5). Metabolite profiling and analysis

were performed at OWL metabolomics. In brief, three separate ultra-performance liquid chromatography–mass spectrometry based platforms were used for optimal profiling of: (1) Fatty acyls, bile acids and lysoglycerophospholipids, (2) Amino acids, and (3) Glycerolipids, cholesteryl esters, sphingolipids, and glycerophospholipids as described(Barr et al., 2012). For these analyzes, 5 independent biological replicates for each group were used, with each replicate consisting of several sets of nerves obtained from different mice. The number of mice used for each replicate was on average: *Gnmt*$^{+/+}$ mice (5) and *Gnmt*$^{-/-}$ mice (5).

Enrichment analysis of TF binding sites. To determine over-represented transcription factor-binding sites, hypomethylated 1-kb tiling regions were screened for the presence of binding sites using Genomatix RegionMiner (http://www.genomatix.de). The number of binding site motifs was determined and over-representation over the background of random mammalian promoter sequences was calculated as the Z-score. Transcription factor matrices with a Z-score greater than 8.0 were considered highly significant.

DNA methytransferase and demethylase activity. Activity of total DNMT and DNA demethylase activity were measured using EpiQuik DNA Methyltransferase Activity/Inhibition Assay Kit and EpiQuik DNA Demethylase Activity/Inhibition Assay Kit respectively (Epigentk), using nuclear fractions of nerves obtained using the Proteoextract Subcellular Proteome Extraction kit (Calbiochem), according to manufacturers protocols. For these analyzes, 4

independent biological replicates for each group were used. The number of mice used for each replicate was on average: NB (20), P10 (10) and P60 (5).

Statistical Analyses. For RRBS analysis, Identification of differentially methylated regions was performed by Methylkit, and a tile or genomic regions were considered to be differentially methylated if it both had a methylation difference of ≥20% between two stages and was significant in a two-sample *t*-test with unequal variance after correction for multiple hypothesis testing (FDR or *q*-value <0.05) using the Benjamini–Hochberg method. For gene expression micro-arrays, data was analyzed as described previously(Iruarrizaga-Lejarreta et al., 2012). In brief, data were processed and normalized using Lumi bioconductor package. For the detection of differentially expressed genes, a linear model was fitted to the data and empirical Bayes moderated t statistics were calculated using the limma package from Bioconductor. Adjustment of p values was done by the determination of false discovery rates using Benjami–Hochberg procedure. For other pair-wise statistical analyses (e.g. qPCR, metabolites measurements), *Student´s t-test* was used and calculated using Microsoft Excel or GraphPad softwares.

SUPPLEMENTAL REFERENCES

Akalin, A., Kormaksson, M., Li, S., Garrett-Bakelman, F.E., Figueroa, M.E., Melnick, A., and Mason, C.E. (2012). methylKit: a comprehensive R package for the analysis of genome-wide DNA methylation profiles. Genome Biol *13*, R87.
Barr, J., Caballeria, J., Martinez-Arranz, I., Dominguez-Diez, A., Alonso, C., Muntane, J., Perez-Cormenzana, M., Garcia-Monzon, C., Mayo, R., Martin-Duce, A., *et al.* (2012). Obesity-dependent metabolic signatures associated with nonalcoholic fatty liver disease progression. J Proteome Res *11*, 2521-2532.
Bock, C., Beerman, I., Lien, W.H., Smith, Z.D., Gu, H., Boyle, P., Gnirke, A., Fuchs, E., Rossi, D.J., and Meissner, A. (2012). DNA methylation dynamics during in vivo differentiation of blood and skin stem cells. Mol Cell *47*, 633-647.
Gu, H., Smith, Z.D., Bock, C., Boyle, P., Gnirke, A., and Meissner, A. (2011). Preparation of reduced representation bisulfite sequencing libraries for genome-scale DNA methylation profiling. Nat Protoc *6*, 468-481.
Halachev, K., Bast, H., Albrecht, F., Lengauer, T., and Bock, C. (2012). EpiExplorer: live exploration and global analysis of large epigenomic datasets. Genome Biol *13*, R96.
Iruarrizaga-Lejarreta, M., Varela-Rey, M., Lozano, J.J., Fernandez-Ramos, D., Rodriguez-Ezpeleta, N., Embade, N., Lu, S.C., van der Kraan, P.M., Blaney Davidson, E.N., Gorospe, M., *et al.* (2012). The RNA-binding protein human antigen R controls global changes in gene expression during Schwann cell development. J Neurosci *32*, 4944-4958.
Jones, P.A. (2012). Functions of DNA methylation: islands, start sites, gene bodies and beyond. Nat Rev Genet *13*, 484-492.
Lee, J.H., Cox, D.J., Mook, D.G., and McCarty, R.C. (1990). Effect of hyperglycemia on pain threshold in alloxan-diabetic rats. Pain *40*, 105-107.
Martinez-Chantar, M.L., Vazquez-Chantada, M., Ariz, U., Martinez, N., Varela, M., Luka, Z., Capdevila, A., Rodriguez, J., Aransay, A.M., Matthiesen, R., *et al.* (2008). Loss of the glycine N-methyltransferase gene leads to steatosis and hepatocellular carcinoma in mice. Hepatology *47*, 1191-1199.
McLean, C.Y., Bristor, D., Hiller, M., Clarke, S.L., Schaar, B.T., Lowe, C.B., Wenger, A.M., and Bejerano, G. (2010). GREAT improves functional interpretation of cis-regulatory regions. Nat Biotechnol *28*, 495-501.
Pande, M., Hur, J., Hong, Y., Backus, C., Hayes, J.M., Oh, S.S., Kretzler, M., and Feldman, E.L. (2011). Transcriptional profiling of diabetic neuropathy in the BKS db/db mouse: a model of type 2 diabetes. Diabetes *60*, 1981-1989.
Shen, Y., Yue, F., McCleary, D.F., Ye, Z., Edsall, L., Kuan, S., Wagner, U., Dixon, J., Lee, L., Lobanenkov, V.V., *et al.* (2012). A map of the cis-regulatory sequences in the mouse genome. Nature *488*, 116-120.
Sullivan, K.A., Lentz, S.I., Roberts, J.L., Jr., and Feldman, E.L. (2008). Criteria for creating and assessing mouse models of diabetic neuropathy. Curr Drug Targets *9*, 3-13.
Woodhoo, A., Alonso, M.B., Droggiti, A., Turmaine, M., D'Antonio, M., Parkinson, D.B., Wilton, D.K., Al-Shawi, R., Simons, P., Shen, J., *et al.* (2009). Notch controls embryonic Schwann cell differentiation, postnatal myelination and adult plasticity. Nat Neurosci *12*, 839-847.